1 Title

- 2 Quantifying the drivers of ecosystem fluxes and water potential across the soil-plant-atmosphere
- 3 continuum in an arid woodland

4

- 5 Authors
- 6 Steven A. Kannenberg<sup>1,2\*,</sup> Mallory L. Barnes<sup>3</sup>, David R. Bowling<sup>2</sup>, Avery W. Driscoll<sup>2,4</sup>, Jessica S. Guo<sup>5</sup>,
- 7 William R.L. Anderegg<sup>2,6</sup>

8

- 9 <sup>1</sup>Department of Biology and Graduate Degree Program in Ecology, Colorado State University, Fort
- 10 Collins, CO, USA
- 11 <sup>2</sup>School of Biological Sciences, University of Uvtah, Salt Lake City, UT, USA
- 12 <sup>3</sup>O'Neill School of Public and Environmental Affairs, Indiana University, Bloomington, IN, USA
- 13 <sup>4</sup>Soil and Crop Sciences, Colorado State University, Fort Collins, CO, USA
- 14 <sup>5</sup>Arizona Experiment Station, University of Arizona, Tucson, AZ, USA
- 15 <sup>6</sup>Wilkes Center for Climate Science and Policy, University of Utah, Salt Lake City, UT, USA
- 16 \*Corresponding author, Steve.Kannenberg@colostate.edu. 612-578-9551

17

- 18 Keywords
- 19 gross primary productivity, evapotranspiration, net ecosystem exchange, piñon-juniper woodland,
- 20 precipitation pulse, water potential

2122

23

24

25

26

27

28

29

30

31

32

33

34

35

36

37

38

39

40

Abstract

Dryland ecosystems occupy a vast swath of the terrestrial land surface and exert a sizeable impact on the cycling of carbon and water globally. These biomes are characterized by tightly coupled carbon and water cycles that respond rapidly to transient pulses in water availability. However, there exist many mechanistic uncertainties regarding the environmental drivers of, and linkages between, plant and ecosystem processes. Thus, drylands are often poorly represented in many vegetation and land surface models. An enhanced understanding of dryland ecosystem function is limited by the lack of long-term, co-located, and frequent measurements of plant and ecosystem processes. At a piñonjuniper woodland in southeastern Utah, USA, we collected a continuous dataset of meteorological conditions, soil water potential from surface to bedrock, tree water potential, and ecosystem carbon and water fluxes from eddy covariance. We found that predawn and midday tree water potential and daily ecosystem fluxes were highly sensitive to fluctuations in soil water availability, particularly in shallower layers, and that daytime variability in atmospheric drivers only loosely controlled these processes. The strong connections between shallow soil water potential, tree water potential, and ecosystem fluxes occurred because of the dominant role of precipitation pulses in driving vegetation activity, as even small pulses of moisture stimulated shallow soil water potential, tree water potential, and evapotranspiration for between 1 and 2 weeks. Carbon fluxes (net ecosystem exchange and gross primary productivity) were sensitive to precipitation pulses for longer, up to 3 weeks. Our results highlight that improved monitoring and sensing of shallow soil moisture can greatly enhance our

understanding of dryland ecosystem function. A better mechanistic understanding of the impacts of precipitation pulses is also needed to improve vegetation modeling of dryland ecosystems.

## Introduction

Semi-arid and arid ecosystems (collectively, "drylands") cover ~40% of the land surface (Reynolds et al., 2007) and are important drivers of interannual variability in the strength of the land carbon sink (Ahlstrom et al., 2015; Poulter et al., 2014). These ecosystems are also generally warm and water-limited (Ehleringer et al., 1999; Noy-Meir, 1973), and thus variability in temperature and water availability exerts a large influence on ecosystem functioning (Forzieri et al., 2011). Such acute water limitation during most of the year results in a tight coupling of water availability and ecosystem fluxes (Wang et al., 2015). Thus, these systems are often characterized by highly 'flashy' ecosystem processes: rapid pulses of carbon and water cycling during conditions that are conducive to vegetation activity (Lauenroth and Bradford, 2009; Schwinning and Sala, 2004). These pulses of activity, though infrequent, exert outsized influence in determining interannual variability in dryland ecosystem fluxes (Kannenberg et al., 2020). Understanding ecosystem processes in drylands is crucial to forecast changes in global carbon cycling, but we currently lack understanding of: 1) the relative importance of various environmental drivers during dynamic ecohydrological conditions, and 2) how to best represent these transient ecosystem processes in vegetation models.

Much of the uncertainty regarding the drivers of dryland carbon-water cycling is due to a poor understanding of the interactions between transient pulses of moisture, atmospheric drivers, soil hydrology, and plant physiology (Gebauer and Ehleringer, 2000; Huxman et al., 2004b; Vargas et al., 2018). While global analyses have found a dominant role for soil moisture in controlling carbon and water fluxes, either through direct limitation on leaf-level fluxes or through indirect feedbacks on atmospheric aridity (Green et al., 2019; Humphrey et al., 2021; Liu et al., 2020), these approaches largely rely on modeled or remotely-sensed proxies for carbon-water cycling that often underestimate the sensitivity of ecosystems to water stress (Kolus et al., 2019; Stocker et al., 2019). Analyses using direct observations of ecosystem fluxes have provided further insights, revealing that the importance of soil versus atmospheric processes is highly variable across ecosystems and depends on site aridity (Fu et al., 2022; Novick et al., 2016). In particular, there is an emerging view that soil moisture is the dominant driver of ecosystem function in drylands. This body of research, however, typically does not consider the role of deep soil moisture pools, which are infrequently measured yet can be crucial for vegetation function (Goulden and Bales, 2019; McCormick et al., 2021; Samuels-Crow et al., 2020).

In addition to uncertainties regarding the environmental drivers of vegetation activity, the impacts of highly transient hydrological conditions (i.e., precipitation pulses) on vegetation are also poorly characterized. Episodic rainfall events in drylands strongly influence biogeochemical cycling and are a primary control of the biogeography, physiology, and demography of vegetation (Forzieri et al., 2011; Noy-Meir, 1973; Reynolds et al., 2004). Research regarding the influence of precipitation pulses on biogeochemical fluxes has mostly been conducted at the plot scale rather than the ecosystem scale (though see Feldman et al., 2021 and Huxman et al., 2004a), and has rarely quantified the direct links between soil, plant, and ecosystem processes simultaneously. As such, it is no wonder that the highly heterogeneous fluxes in dryland ecosystems are poorly represented in the land surface components of Earth system models, which commonly fail to capture both the variability and magnitude of carbon and water cycling (Barnes et al., 2021; MacBean et al., 2021; Smith et al., 2019; Verma et al., 2014). The reasons for this are numerous but include: 1) model inability to capture highly variable soil moisture dynamics across depths (MacBean et al., 2020), and 2) unknowns regarding the mechanistic responses of vegetation to rapid fluctuations in atmospheric aridity and soil moisture (Roby et al., 2020).

Our mechanistic understanding of dryland ecosystem processes is also in part limited by the types of long-term, continuous data available. While remotely-sensed and modeled data provide insight into the drivers of broad-scale vegetation activity, their uncertainty at finer spatial and temporal resolutions makes them less suitable for uncovering ecosystem dynamics in biomes driven by transient pulses of moisture. Eddy covariance networks (e.g., AmeriFlux (Novick et al., 2018) and FLUXNET (Pastorello et al., 2020) have substantially improved our ability to evaluate ecosystem carbon-water dynamics, but these datasets do not always contain the primary environmental drivers of ecosystem fluxes (e.g., soil moisture), nor do they typically provide any measurements of vegetation physiology. Because plant hydraulic function plays a critical role in mediating ecosystem fluxes (Anderegg et al., 2018; Eller et al., 2020; Sabot et al., 2020), more widespread and continuous measurements of plant hydraulic status have the potential to enhance our knowledge of the drivers of ecosystem fluxes. However, most plant water potential measurement methods are destructive and time-consuming, limiting their applicability for understanding ecosystem processes at faster temporal scales. Methods to continuously monitor plant water potential show promise in this regard but are not yet widely deployed (Guo et al., 2020; Jain et al., 2021; Novick et al., 2022). When collected at eddy covariance tower sites, these high-frequency water potential measurements have the potential to shed key insights into the mechanistic linkages between the responses of individual plants and whole ecosystem fluxes.

Further understanding of the interactions between precipitation, atmospheric demand, belowground hydrology, and vegetation physiology in drylands will help better constrain our understanding of carbon-water cycling and improve our projections of ecosystem function in these regions as they get warmer and drier (Cook et al., 2021). Towards this aim, we collected a 3-year dataset of co-located measurements of soil water potential, ecosystem fluxes, and meteorological drivers in a piñon-juniper woodland in southeastern Utah. We additionally amassed a continuous (half-hourly) dataset of plant water potential for the dominant species, *Juniperus osteosperma*, during one of those growing seasons. Our goals were to: 1) uncover the primary drivers of plant water potential and ecosystem fluxes, 2) characterize the dynamic interrelationships between plant and soil hydraulics and ecosystem fluxes at this site, and 3) understand the impact of precipitation pulses on ecosystem function.

## Methods

Site

The study site is located at 37.5241, -109.7471 in southeastern Utah at 1866 m elevation. The region experiences a cold semi-arid climate (Köppen climate type: BSk), with cold winters and hot, dry summers. The site is at the northern edge of the North American Monsoon boundary, which leads to high interannual variability in precipitation. Mean May – October precipitation is  $159 \pm 47$  mm (standard deviation) while mean November – April precipitation is  $160 \pm 61$  mm. The area surrounding the site is relatively flat, with the nearest large topographical feature ~1.2 km away.

The vegetation is characteristic of an early successional piñon-juniper woodland, primarily composed of Utah juniper (*Juniperus osteosperma*, which comprises 92% of total tree basal area) and two-needle piñon (*Pinus edulis*, comprising 8% of tree basal area), with an average tree height of ~3 m. The understory is sparse, with occasional big sagebrush (*Artemesia tridentata*), prickly pear cactus (*Opuntia* spp.), and various bunchgrasses. This land was chained (i.e., all aboveground vegetation was mechanically removed) in the 1960s, and thus the site is at a much earlier successional stage with lower tree density (11.71 m²/ha tree basal area) than the surrounding late- and mid-successional piñon-juniper woodland (~24 m²/ha tree basal area). The soil is a sandy loam, with a highly variable fractured bedrock

layer that is on average 1.4 m deep, but can vary between 0.25 m and 2 m (Nauman and Duniway, 2020).

## Eddy covariance tower instrumentation and data processing

In June 2019, an eddy covariance flux tower (AmeriFlux site ID: US-CdM, Kannenberg et al., 2022) was deployed at this site to measure fluxes of energy, carbon, and water, as well as to monitor other meteorological variables. The eddy covariance instrumentation included: a Campbell Scientific CSAT3 sonic anemometer and Campbell Scientific EC150 open-path infrared gas analyzer, a Vaisala HMP155 temperature and relative humidity sensor, a Kipp and Zonen CNR4 net radiometer, an upfacing Kipp and Zonen PQS1 photosynthetic photon flux density (PPFD) sensor, and a Campbell Scientific TE535WS tipping bucket rain gauge. The sonic anemometer, gas analyzer, and temperature/humidity instruments were installed at a height of 8 m, while the net radiometer and PPFD sensors were installed at a height of 6.45 m. Five Acclima TDT soil temperature and volumetric water content sensors were also deployed underneath the tower from surface to bedrock, at depths of 5 cm, 10 cm, 20 cm, 50 cm, and 100 cm. All instruments were factory-calibrated prior to deployment, and the gas analyzer was calibrated via a zero-span procedure approximately every 4 months. Data from these maintenance periods were removed, which typically lasted for between 3 and 6 hours. We note that measurements of precipitation during the winter are likely inaccurate due to the inability of tipping-bucket rain gauges to accurately measure snow. Rain gauge data are presented in Fig. S1 for context but are not used in any analyses.

To convert measurements of volumetric water content to soil water potential ( $\Psi_{\text{soil}}$ ), a water retention curve was developed using a METER Group WP4 dewpoint potentiometer (Fig. S2). Briefly, soil samples were fully dried, and drops of water were added to 8 subsamples to generate a range of volumetric water contents from 0 – 30%. These samples were sealed and allowed to equilibrate for 24 hours in a refrigerator, after which they were brought to room temperature.  $\Psi_{\text{soil}}$  was then measured via the WP4 and gravimetric water content was determined by weighing the samples before and after the addition of water. Gravimetric water content was converted to volumetric water content using measurements of soil bulk density. Using these measurements of  $\Psi_{\text{soil}}$  and volumetric water content, parameters for the van Genuchten (1980) curve equation were estimated using the online SWRC tool (Seki, 2007). Water retention curves were replicated twice each on soil collected from two different depths (0 – 10 cm and 30 – 50 cm), and all data were used to determine the final curve parameters since there was no appreciable difference in the water retention curves across depths. The root mean square error between values predicted by this moisture retention curve and measured values was 2.08 MPa and the R² was 0.77.

High frequency eddy covariance data were processed into half-hourly values of net ecosystem exchange (NEE) using the Campbell Scientific program *EasyFlux PC*. Data were first de-spiked using the Vickers and Mahrt (1997) method, and coordinate rotation was performed using a planar fit. The Massman spectral correction (Massman, 2000) and Webb-Pearman-Leuning density correction (Webb et al., 1980) were then applied. For meteorological variables, data were processed into half-hourly means (or sums for precipitation). Following this initial data processing, NEE was gap-filled using the 50<sup>th</sup> percentile u\* distribution (Pastorello et al. 2020) and then partitioned into gross primary productivity (GPP) and ecosystem respiration (RE) using the nighttime method (Reichstein et al., 2005), as implemented in the R package *REddyProc* (Wutzler et al., 2018). Air temperature (TA), vapor pressure deficit (VPD), and incoming shortwave radiation were gap-filled using the Marginal Distribution Sampling (MDS) algorithm (Reichstein et al., 2005). Since our primary objective was to isolate the drivers of ecosystem function, we constrained our data record to the warm season (May – October) and daytime

(9 am - 5 pm). We then aggregated half-hourly data to daily means, or sums where appropriate (i.e., ecosystem fluxes and precipitation).

## Stem psychrometer instrumentation and data processing

On May 24, 2021, 14 ICT PSY1 automated stem psychrometers were installed on Utah juniper trees within 20 m of the flux tower. Stem psychrometers measure xylem water potential through a dual-thermocouple design that generates wet bulb depression and corrects for temperature gradients in the chamber. Since this method is minimally destructive, it can be used to obtain a continuous time series of stem water potential. All instruments were calibrated prior to installation in the field, as per the manufacturer's instructions. Briefly, solutions of potassium chloride were created that correspond to water potentials of 0.46, 0.91, 1.37, 1.82, 2.28, 4.64, and 6.9 MPa. Filter paper discs were soaked in each solution and placed in a metal cap, which was sealed on to the psychrometer chamber with a small amount of vacuum grease. The water vapor in the psychrometer chamber was then allowed to equilibrate with the solution on the disc for at least 30 min, after which a water potential measurement was taken. The procedure was then repeated for the remaining solutions. The slope and y-intercept between measured and actual water potential were applied to each psychrometer; calibrations were rerun if the R<sup>2</sup> of this linear fit was below 0.99.

Seven mature, healthy trees (between 2 and 3 m in height) were selected, and 2 psychrometers were installed on different branches within each tree. Psychrometers were installed as per the manufacturer's instructions, by removing bark and phloem with a flat knife, cleaning the exposed xylem with water and a cloth, and attaching the instrument chamber to the exposed xylem with a clamp. The psychrometer chambers were further secured to the branch with self-adhesive silicone tape to ensure a tight seal and covered in a reflective and watertight radiation shield to minimize temperature fluctuation and keep the instruments (along with any exposed xylem external to the instrument chamber) dry. The psychrometers were then set to take one measurement every 30 minutes and remained installed until November 5, 2021.

Stem psychrometer data are only accurate when there is a tight seal between the chamber and the exposed xylem. Thus, the wounding response of plants can impact the validity of the data and psychrometers cannot be installed indefinitely. Every 4-5 weeks (5 times throughout the study period), all psychrometers were uninstalled, organic material (wood, resin, etc.) was removed from the sensor using chloroform and water, the chamber was gently dried with compressed air, and the psychrometers were reinstalled on new branches. This reinstallation period was chosen to reflect the average time that these instruments remained functional. No branch was used twice over the entire study period. One day after each reinstallation period, psychrometer-derived stem water potential data were validated with traditional pressure chamber measurements via a PMS Instruments Model 610 Scholander pressure chamber (Fig. S3, p < 0.0001,  $R^2 = 0.58$ ). On each of these days, two such water potential measurements were conducted on each tree that the psychrometers were installed on (total of n = 14 for each day). We do note that the psychrometer-derived measurements of tree water potential were more negative than those derived from the pressure chamber during extremely dry conditions (Fig. S3), though the exclusion of these values (< -6 MPa) do not alter our conclusions.

Stem water potential data were visually assessed to screen for measurement artifacts and errors. Our criteria for removing data were as follows: 1) during maintenance/cleaning periods, and for 1 day following these periods, 2) outliers that were > 0.5 MPa away from adjacent points, 3) after any sizeable 'step change' in the magnitude of measured stem water potential that could not be attributed to a precipitation event, and 4) any time a diurnal cycle in water potential was lost. This data processing

procedure resulted in quality data being available for 10 stem psychrometers on average at a given moment, with at least half of the psychrometers active during 93% of the study period. Following this data processing, water potential data were aggregated into daily stand-level means during predawn (2 - 4 am) and midday (1 - 3 pm) periods.

# Quantifying precipitation pulses

The impact of precipitation events on ecosystem processes was quantified by standardizing (z-scoring) all variables, identifying > 2 mm precipitation events, and conducting a Superposed Epoch Analysis (SEA) via the sea function in the R package dplR (Bunn, 2008). This technique involves a bootstrapping approach (n = 1000) to determine if the variable in question is significantly different from its baseline variability during the 30 days following the precipitation event (or until the next precipitation event if it occurred within that 30-day period). When concurrent precipitation days occurred, only the last day was included in our analysis. We elected to use a threshold of > 2 mm precipitation to identify a rain event, as this value struck a balance between impact and rarity (14 events during the study period). Our results were functionally equivalent when using different thresholds for daily precipitation (Fig. S4-S5), including 1 mm (n = 19) and 3 mm (n = 9). We also used locally estimated scatterplot smoothing (LOESS regression) with 95% confidence intervals and a span of 0.5 on these scaled variables to provide a way of visualizing and validating this method. All analyses were conducted in R version 4.0.4 (R Core Team, 2022).

#### **Results**

Responses of  $\Psi_{stem}$  and ecosystem fluxes to site climate variability

During the study period (May 2019 to November 2021), this site displayed a climate characteristic of high desert ecosystems: cold winters followed by warm, dry summers with high light availability (Fig. S1). However, these years were characterized by three markedly divergent hydrologic regimes. The summer of 2019 was generally wet, followed by a winter with frequent precipitation and a snowpack accumulation of 5-19 cm that persisted for nearly two months, which recharged deep (50-100 cm) layers of soil moisture in the spring during snowmelt. The summer of 2020, however, was hot and dry, coinciding with the initiation of a D3-level ('extreme') drought in August (U.S. Drought Monitor) that developed into a D4-level ('exceptional') drought by November. Late summer precipitation in 2020 was minimal, as was snowpack accumulation during the subsequent winter. As a result, deep soil moisture pools were not recharged in the spring of 2021. Summer 2021, when measurements of  $\Psi_{\text{stem}}$  took place, started out dry and continued to get drier until mid-July, when monsoonal rains caused large fluctuations in  $\Psi_{\text{soil}}$  in the upper (above 20 cm) layers. During 2021, the site continued to switch between D3- and D4-level drought. Fluxes of carbon and water generally tracked fluctuations in water availability – peaking in the late spring and during the monsoon season, when present (Fig. 1).

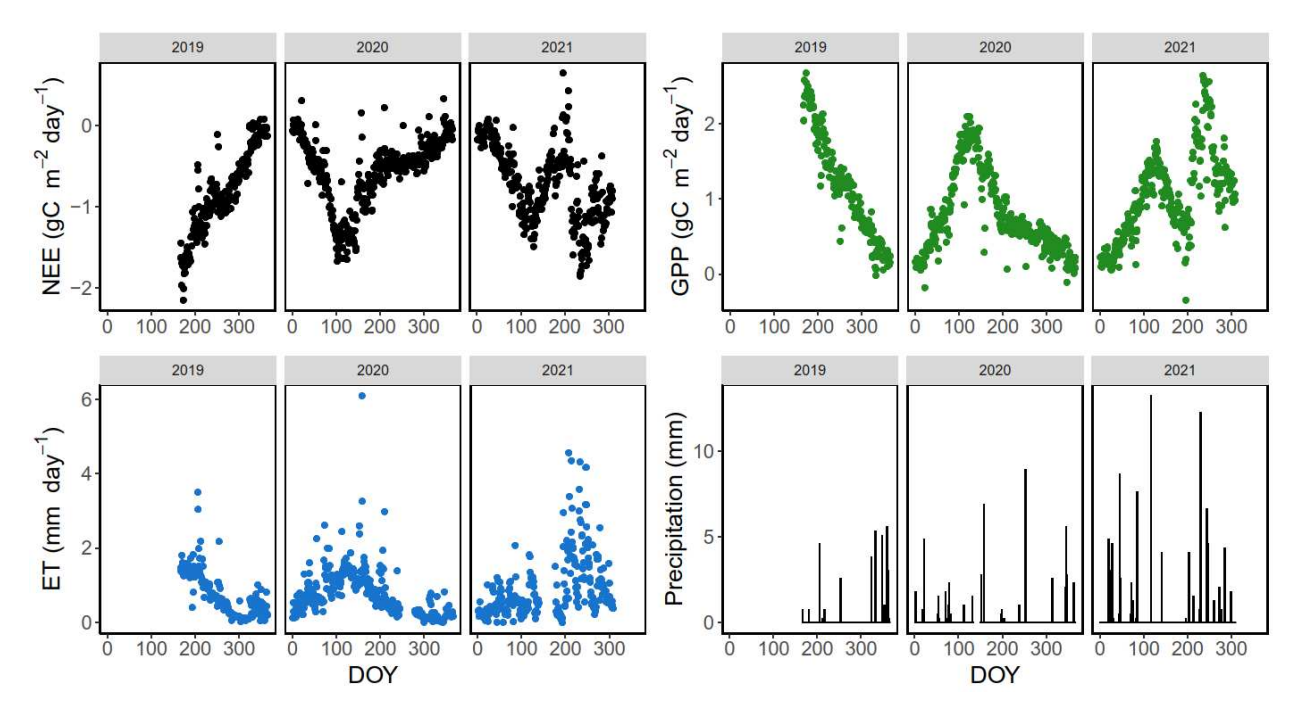


Fig 1. Time series of daily summed ecosystem fluxes (NEE, GPP, and ET) and precipitation.

Predawn and midday  $\Psi_{\text{stem}}$  were highly dynamic during 2021, slowly decreasing during the early-and mid-summer (DOY 144 – 208) before rapidly increasing due to monsoonal rains in mid-July on DOY 209 (Fig. 2). Following this initial pulse of water availability, predawn/midday  $\Psi_{\text{stem}}$  rapidly decreased in mid-September (DOY 257 – 267), before rising again due to another precipitation pulse, where it remained high until the end of the measurement period in November. Variability in stem water potential across all measured branches increased during these dry periods, whereas stem water potential was more consistent across trees during wetter periods (Fig. S6-S7).

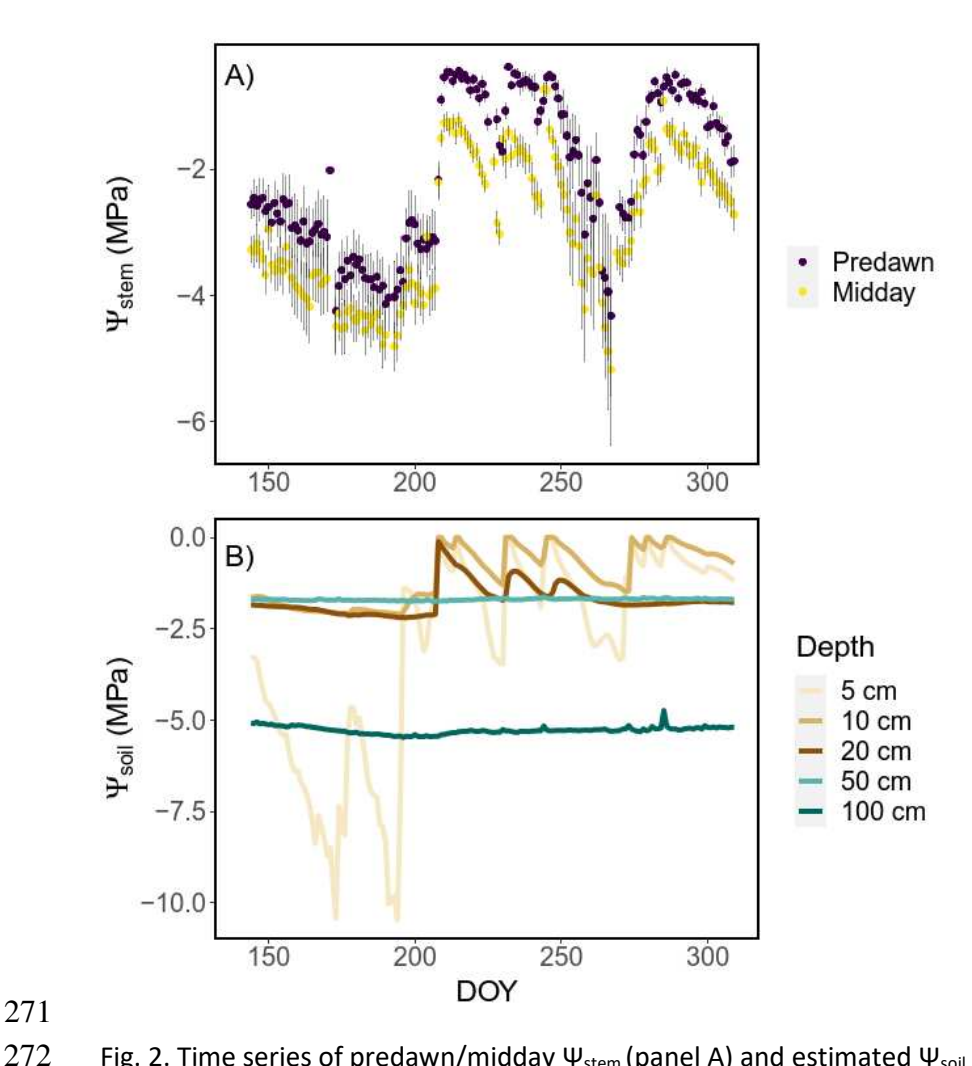


Fig. 2. Time series of predawn/midday  $\Psi_{\text{stem}}$  (panel A) and estimated  $\Psi_{\text{soil}}$  (panel B) during May-November 2021.

Linkages between environmental drivers, ecosystem fluxes, and  $\Psi_{\text{stem}}$ 

Daily fluxes of carbon and water, as well as predawn/midday  $\Psi_{\text{stem}}$ , were highly sensitive to  $\Psi_{\text{soil}}$ variability in shallow and middle layers (Fig. 3). Carbon fluxes (NEE and GPP) were most sensitive to Ψ<sub>soil</sub> in 20 cm and 50 cm layers, while evapotranspiration and predawn/midday Ψ<sub>stem</sub> correlation coefficients were highest for shallower (5 cm, 10 cm, and 20 cm) layers. In contrast, the sensitivity of ecosystem processes to atmospheric drivers (TA, VPD, incoming PPFD) was much weaker. Results were similar when considering data aggregated at the half-hourly scale, as well as when using soil volumetric water content instead of  $\Psi_{soil}$  (Fig. S8-S9). Predawn and midday  $\Psi_{stem}$  was also significantly coupled to daily NEE, GPP, and ET (Fig. 4), and despite many additional confounding factors in the half-hourly data, correlations were still significant, albeit weaker (Fig. S10). Due to the divergent seasonal cycles of atmospheric aridity versus soil moisture, VPD and  $\Psi_{\text{soil}}$  in any layer were only weakly correlated to each other on both half-hourly (p < 0.01, maximum  $R^2$  = 0.15) and daily (p < 0.01, maximum  $R^2$  = 0.19) time scales.

271

273

274 275

276

277

278

279

280

281

282

283

284

285



Fig. 3. Correlation matrix for linear regressions between daily ecosystem fluxes, predawn/midday  $\Psi_{\text{stem}}$ , and various environmental drivers. Numbers, color, and size of points represent the Pearson's correlation coefficient between two variables. For correlations with fluxes, environmental drivers were aggregated to daily means, and for correlations with water potential, environmental drivers were the mean of observed values during the specified time period (predawn or midday). Only significant ( $\alpha$  = 0.05) correlations are shown. Results for ecosystem fluxes and environmental drivers encompass the growing seasons from 2019 – 2021, while results for predawn/midday  $\Psi_{\text{stem}}$  pertain to the psychrometer measurement period (May 2021 – November 2021).

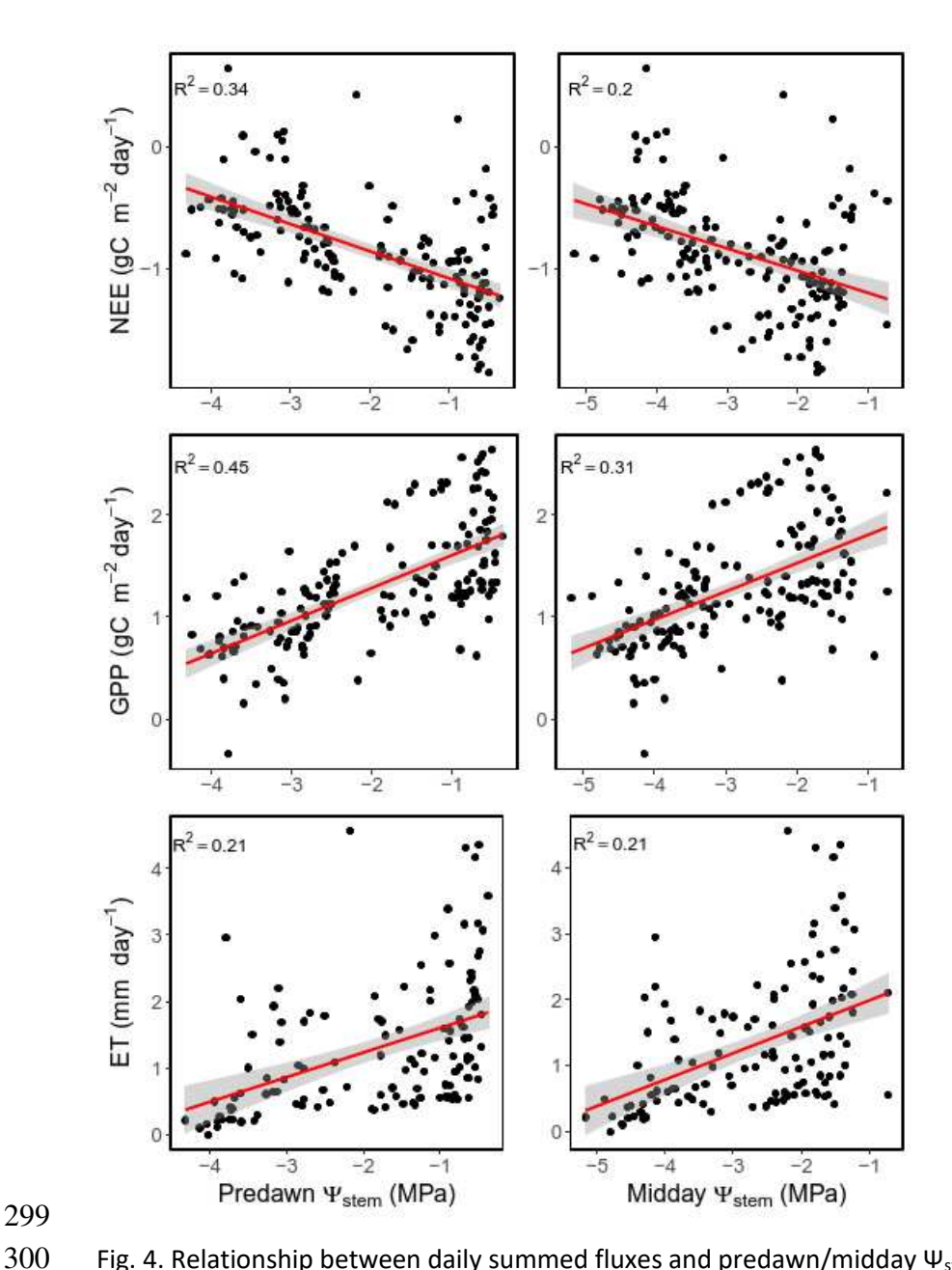


Fig. 4. Relationship between daily summed fluxes and predawn/midday  $\Psi_{\text{stem}}$  from May 2021 – November 2021. Linear regressions (plus 95% confidence bands) are indicated in red. All regression p-values are less than 0.001.

## Impact of precipitation pulses on carbon and water cycling

Precipitation pulses (> 2 mm rainfall during a given day) were found to have a sizeable and long-lasting impact on ecosystem function (Fig. 5, Table S1). Following a rain event, shallow  $\Psi_{\text{soil}}$  (in 5 cm and 10 cm layers) and ET were significantly stimulated for between 11 and 14 days, while deeper soil layers were unchanged. Predawn and midday  $\Psi_{\text{stem}}$  were also stimulated, though after a lag of 4 – 5 days and for a much shorter time period of 3 – 4 days. Carbon fluxes (NEE and GPP) were stimulated for longer, between 21 and 22 days. These stimulations were not always instant, however. For example, GPP was suppressed during the precipitation day, and took 1-day post-precipitation to become stimulated,

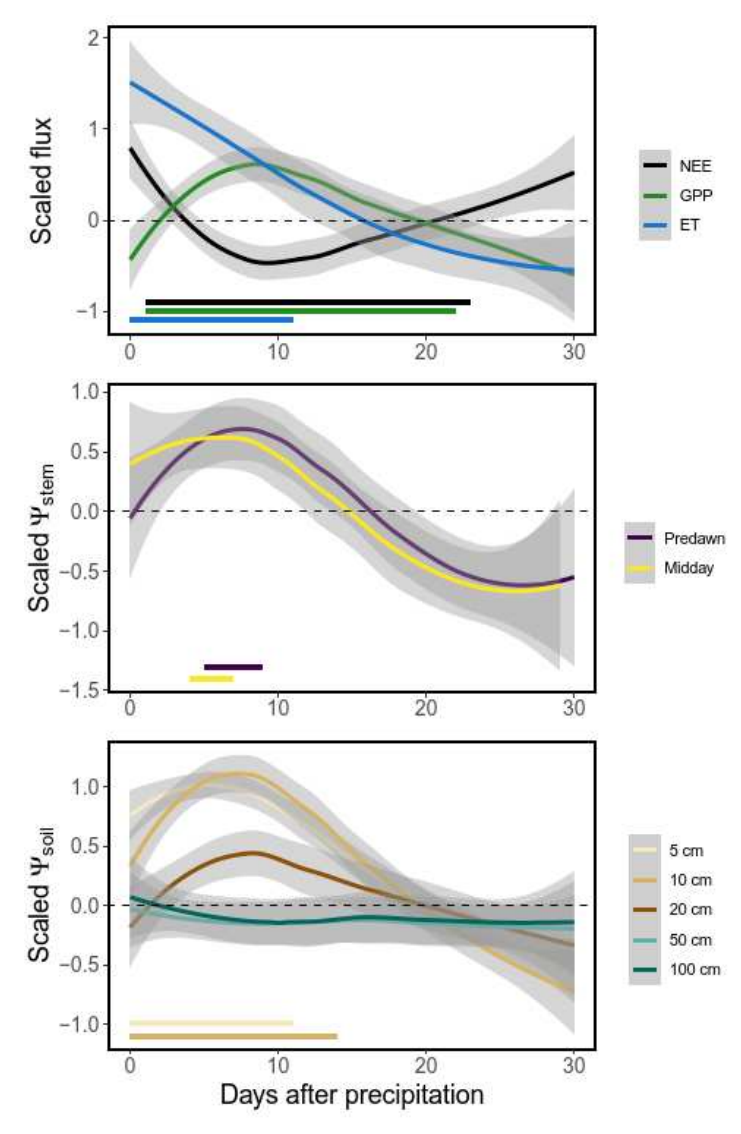


Fig. 5. Smoothed time series (plus 95% confidence bands) for all measured ecosystem processes following a > 2 mm precipitation event. All variables are scaled, and thus the dotted line at 0 represents the mean value for that variable across the entire measurement period. The color bars at the bottom of each graph represent the period of time when the indicated process was significantly ( $\alpha$  = 0.05) affected following the precipitation event, as calculated via Superposed Epoch Analysis (SEA). Results for ecosystem fluxes and  $\Psi_{\text{soil}}$  encompass May 2019 – November 2021, while results for predawn/midday  $\Psi_{\text{stem}}$  pertain to the psychrometer measurement period (May 2021 – November 2021).

The influence of atmospheric drivers versus  $\Psi_{soil}$  on ecosystem function

Ecosystem processes in this piñon-juniper woodland were highly sensitive to variability in shallow-medium soil moisture pools derived from small summer precipitation events. While it is intuitive that this ecosystem should be limited by soil water availability, the degree to which shallow-medium soil moisture controlled water potential and fluxes was surprising, especially given: 1) the central role of vapor pressure deficit in regulating vegetation activity in many systems (Grossiord et al., 2020), and 2) the reputation of Utah juniper as a deeply rooted species that is insensitive to fluctuations in shallow moisture (Schwinning et al., 2020; West et al., 2007b, 2007a).

While it has been found that arid ecosystems are more sensitive to soil moisture than to vapor pressure deficit (Novick et al., 2016), it is surprising that correlations between ecosystem process and atmospheric drivers at this site were so weak, and frequently non-existent. We hypothesize that this is due to a decoupling between water availability and the seasonal cycles of temperature, light, and vapor pressure deficit. Water availability and carbon-water fluxes at this site peaked during two periods: 1) late spring to early summer, when snowmelt-derived deep moisture pools were more plentiful, and 2) late summer, when North American Monsoon-derived precipitation was present. Notably, these two periods have divergent atmospheric conditions – cooler, wetter, and darker in the late spring and early summer, and vice versa for the late summer. It was this divergence in atmospheric drivers versus soil water availability that likely obscured the link between VPD and ecosystem fluxes.

A strong dependence of ecosystem function on soil moisture has important implications for vegetation modeling. Many models represent soil moisture stress via highly-simplified functions that lack an empirical basis (Trugman et al., 2018). Such a tight coupling between shallow moisture and ecosystem fluxes is likely to underlie the poor performance of many land surface models in the southwestern United States, as highly dynamic water supply in shallow layers is frequently one of the largest uncertainties in vegetation models (MacBean et al., 2020). Our results highlight the need to better represent transient surface soil hydrology, as well as deeper soil moisture pools. Fortunately, recently developed plant hydraulics models (e.g., Eller et al., 2020; Sabot et al., 2020; Sperry et al., 2017; Venturas et al., 2020) are a sizeable improvement in the representation of soil moisture dynamics and vegetation responses to fluctuations in water availability. The significant correlations we observed between fluxes and water potential also highlight the utility of these models for scaling from plant physiological principles to ecosystem fluxes. We also note that there is likely noise introduced in these correlations due to fluxes from the co-occurring piñon pines and other understory vegetation, and future plant hydraulic model development should focus on such multi-species interactions. The unique dataset we have amassed here can serve as a valuable tool for benchmarking such models, and will hopefully inspire the collection of similar datasets in other biomes.

The correlations between ecosystem processes and  $\Psi_{soil}$  varied with depth. Correlation coefficients for carbon fluxes (NEE, GPP) tended to peak in the 20 cm layer, consistent with the documented rooting distribution of Utah juniper (Schwinning et al., 2020). Correlation coefficients for evapotranspiration, in contrast, were similar across 5 cm, 10 cm, and 20 cm layers, likely reflecting the combined influence of juniper rooting depth driving transpiration, and the influence of surface soil moisture on evaporation. Predawn/midday  $\Psi_{stem}$  was most strongly correlated with surface (5 cm)  $\Psi_{soil}$ . This was surprising, as we expected similar drivers of carbon fluxes and  $\Psi_{stem}$ . However, this result could be explained by lower variability in 10-20 cm  $\Psi_{soil}$  during the year when stem psychrometers were installed compared to the longer flux tower record. This same explanation likely underpins the non-existent correlations between predawn/midday  $\Psi_{stem}$  and deep  $\Psi_{soil}$ .

Our finding that shallow soil moisture was the dominant control over fluxes at this woodland differs from a nearby semi-arid grassland (US-Cop; Bowling et al. 2010), where deep soil moisture

regulated ecosystem carbon uptake. Aside from vegetation type (C<sub>4</sub> grasses vs. C<sub>3</sub> woody plants), biome (the grassland is warmer, drier, and lower in elevation), and subsurface hydrology (the woodland has shallow and highly variable bedrock depth), much of the soil moisture signal detected at US-Cop occurred in the spring, which falls outside of the definition of the growing season at our woodland site. Furthermore, the southwestern US 'megadrought' (Williams et al. 2022), which had been ongoing for more than 20 years when we took our measurements, could be making transient summer precipitation a more important driver of ecosystem function. Our findings show that during the growing season, a woody dryland biome can be highly responsive to both shallow and deep soil moisture fluctuations, and that the degree to which shallow versus deep soil moisture influences ecosystem function is highly dependent on interannual climate variability.

It is worth noting that variability in stem water potential across branches increased markedly during dry-down periods. This variability could be due to differences in branch microclimate and deep water access, the sectorial nature of the Utah juniper hydraulic system (Schenk et al., 2008), or variability in leaf and sapwood area across branches (Beikircher and Mayr, 2008). While our data do not allow us to disentangle these hypotheses, future investigations using psychrometers or high-frequency pressure chamber measurements could investigate branch-level differences in stem water potential. Such variability is likely to contribute to the challenge of using plant hydraulic models to accurately predict drought impacts (Venturas et al., 2020).

Interannual variability in deep soil moisture pools, and implications for carbon uptake

While shallow soil moisture variability was driven by summer precipitation pulses, deep soil moisture pools seemed to only increase following significant snowmelt in the spring. Due to this sporadic recharge, ecosystem processes were less sensitive to variability in deep soil moisture than shallow soil moisture, though we still did see moderately high correlation coefficients between fluxes and deep  $\Psi_{\text{soil}}$ . While we cannot rule out the possibility that heavy summer or fall rains could percolate to deeper soils (e.g., Bowling et al., 2010), it seems likely that the recharge of deep moisture pools in this region is highly dependent on the accumulation of snowpack and its subsequent melt in the spring.

The southwestern US has recently experienced severe water stress, including long-term reductions in snowpack (Siirila-Woodburn et al., 2021), the ongoing 'megadrought' (Williams et al., 2022), and recent regional droughts in 2018 and 2020 – present (Kannenberg et al., 2021). Despite these droughts, and despite very dry deep soils in 2021, the US-CdM site remained a persistent carbon sink in all 3 years. Many southwestern US ecosystems switch between carbon sources and sinks year to year, though piñon-juniper woodlands tend to be a more consistent carbon sink than other southwestern US ecosystems (Biederman et al., 2017). The consistent carbon sink at US-CdM could also arise from the site's early successional stage due to its land management history (i.e., mechanical vegetation removal  $\sim$ 60 years ago). The future of this sink is unknown and will depend on future climate trends and vegetation activity as the woodland transitions into mid-or late successional stages. Given projections of decreasing winter precipitation and increasing summer aridity across the region (Cook et al., 2021; Siirila-Woodburn et al., 2021), deep soil moisture pools are likely to continue to remain low, and this carbon sink will increasingly depend on the interaction between summer precipitation and vegetation physiology. Unfortunately, there exists the possibility that trees exposed to such long-term drought could lose their capacity to respond to summer precipitation pulses (Plaut et al., 2013), which could further hasten the documented increase in climate-related risks that piñon-juniper woodlands will face in the future (Anderegg et al., 2022).

420

421

422

423

424

425

426

427

428

429

430

431

432

433

434

435

436

437

438

439

440

441

442

443

444

445

446

447

448

449

450

451

452

453

454

455

456

457

458

459

460

461

463

464

The role of shallow soil moisture in mediating ecosystem processes was driven by the impact of small and transient precipitation pulses. Following a rain event, shallow soil moisture and evapotranspiration were immediately stimulated for up to 2 weeks. Carbon fluxes, however, experienced a 1-day lag before they were stimulated, after which they remained elevated for up to 3 weeks. This lag was likely due to: a) the co-occurrence of conditions that suppress photosynthesis during rainy days (e.g., clouds, low temperature), or b) physiological or hydrological lags between water inputs and photosynthesis (Huxman et al., 2004b). Predawn/midday  $\Psi_{\text{stem}}$  was stimulated for a shorter period of time, and exhibited a multi-day lag before the impacts of precipitation were detected. This lag period could also be due to the weather during rainy days or physiological/hydrological lags. However, there were also far fewer precipitation events (5) during the period when  $\Psi_{\text{stem}}$  measurements were conducted, and thus these dynamics may be due to reduced statistical power in our  $\Psi_{\text{stem}}$  dataset relative to the flux tower record. Though, we note that the shape and magnitude of the predawn/midday  $\Psi_{\text{stem}}$  curve following precipitation is similar to that of  $\Psi_{\text{soil}}$ , and given the strong correlations between  $\Psi_{\text{stem}}$  and  $\Psi_{\text{stem}}$  and  $\Psi_{\text{soil}}$  it is likely that predawn/midday  $\Psi_{\text{stem}}$  was actually impacted for weeks.

There is a rich history of research on the impacts of precipitation pulses in dryland ecosystems (e.g., Huxman et al., 2004a; Jenerette et al., 2008; Noy-Meir, 1973; Reynolds et al., 2004). Our results add to this body of work in three ways. First, we found a much higher sensitivity of all ecosystem processes to precipitation pulses than has been previously documented. Most research to date has characterized the impact of precipitation pulses > 5 mm, with a frequent focus on the impact of > 20 mm irrigation treatments (Gebauer and Ehleringer, 2000; West et al., 2007b; Williams and Ehleringer, 2000). Rain events of that size are rare in this region, and as such vegetation might be more adapted to responding to smaller moisture inputs than previously recognized. Moreover, most studies have not statistically quantified the length of time that ecosystem processes were stimulated, and those that do have found much shorter stimulation periods (Feldman et al., 2020, 2021; though see Kurc and Small, 2007). Reynolds et al. (2004) have even suggested that precipitation pulses in drylands are only important insofar as they tend to occur as part of larger storm systems. Given that only one of our precipitation events occurred as part of a larger multi-day precipitation event, coupled with the static nature of mid- and deep-layer moisture following summer precipitation, this explanation is not likely at our site. Second, our results contradict the paradigm that dryland juniper species are less sensitive to shallow soil moisture dynamics due to their deep rooting system (West et al., 2007b, 2007a). Our data indicate that juniper is capable of rapid water uptake in shallower layers - potentially an acclimation to long-term reductions in deep pools of soil moisture. Finally, the difference in length of stimulation between hydrologic processes ( $\Psi_{\text{stem}}$ ,  $\Psi_{\text{soil}}$ , and ET) and carbon fluxes (NEE and GPP) is particularly notable. Photosynthesis does not decline linearly with plant and  $\Psi_{\text{soil}}$ , and only starts to decrease when plant water potential nears key hydraulic thresholds (Sperry et al., 2017). These thresholds (e.g., P50, the xylem water potential at which half of conductivity is lost) are particularly robust for Utah juniper (Koepke and Kolb, 2013), and may underly the long-term stimulation of carbon fluxes following small precipitation events at this site. Such findings likely reflect the influence of recent chronic and acute droughts on ecosystem function (Kannenberg et al., 2021; Williams et al., 2022), and underscore the importance of measuring multiple ecosystem processes in concert.

## 462 Conclusions

Piñon-juniper woodlands in the southwestern United States have been under increasing stress in recent decades, including multiple widespread drought-induced mortality events (Breshears et al.,

2005; Kannenberg et al., 2021). Combined measurements of soil moisture, plant water potential, ecosystem fluxes, and atmospheric drivers will provide insight into how this biome will respond to future climatic changes. Our observations have allowed us to quantify the importance of two distinct soil moisture pools for piñon-juniper ecosystem function a) deep soil moisture derived from snowpack, and b) small and transient pulses of summer precipitation, as well as characterize the tight links between soil moisture, plant hydraulic status, and ecosystem fluxes.

These results demonstrate the progress that can be made towards understanding dryland carbon-water processes by better quantifying the highly transient shallow soil moisture dynamics. If shallow soil moisture is the dominant control on ecosystem function in many drylands, then more advanced soil hydrology models can provide a much-needed improvement to the prediction of dryland carbon-water cycling (MacBean et al., 2021, 2020). Though, more work remains to determine which precipitation pulses meaningfully impact shallow soil moisture, when that influx of water percolates down to mid- or deep-layer soils, and how vegetation responds to these hydrological fluctuations. Progress towards this aim would greatly benefit from larger networks of soil moisture and plant water potential observations (Novick et al., 2022), in addition to remote sensing approaches for quantifying soil moisture across depths (e.g., Soil Moisture Active Passive - SMAP) and broader inclusion of carbonwater coupling in vegetation models and datasets of ecosystem fluxes (Barnes et al., 2021; Kennedy et al., 2019).

## **Acknowledgements**

A special thanks to Dave Eiriksson and Ryan Bares for assistance in setting up the eddy covariance tower, and to Stephen Chan for eddy covariance assistance throughout. The instrumentation for the eddy covariance tower was provided by the AmeriFlux Management Project, administered through the US Department of Energy (DOE). We also thank Newton Tran for assistance with the stem psychrometers, and acknowledge the State of Utah School and Institutional Trust Lands Administration for land permissions. SAK was supported by the US Department of Agriculture (USDA) Forest Service Forest Health Protection Evaluation Monitoring program grant #19-05, the US DOE Environmental System Science program grant #DE-SC0022052, and the USDA National Institute of Food and Agriculture Sustainable Agricultural Systems program, grant #2021-68012-35898. MLB also acknowledges support from US DOE Environmental System Science program grant #DE-SC0022052. DRB acknowledges support from US National Science Foundation (NSF) grants #1929709 and #1926090. AWD acknowledges support from US NSF grant #1828902 and the NSF Graduate Research Fellowship program. WRLA acknowledges support from the David and Lucille Packard Foundation, US NSF grants #1714972, #1802880, #2003017, and #2044937, and USDA National Institute of Food and Agriculture Agricultural and Food Research Initiative Competitive Programme Ecosystem Services and Agro-Ecosystem Management, grant #2018-67019-27850.

#### References

- Ahlstrom, A., Raupach, M.R., Schurgers, G., Smith, B., Arneth, A., Jung, M., Reichstein, M., Canadell, J.G., Friedlingstein, P., Jain, A.K., Kato, E., Pulter, B., Sitch, S., Stocker, B.D., Viovy, N., Wang, Y.P., Wiltshire, A., Zaehle, S., Zeng, N., 2015. The dominant role of semi-arid ecosystems in the tren and variability of the land CO2 sink. Science (80-. ). 348, 4503–4518. https://doi.org/10.1002/2015JA021022
- Anderegg, W.R.L., Chegwidden, O.S., Badgley, G., Trugman, A.T., Cullenward, D., Abatzoglou, J.T., Hicke,

- J.A., Freeman, J., Hamman, J.J., 2022. Future climate risks from stress, insects and fire across US forests. Ecol. Lett. https://doi.org/10.1111/ele.14018
- Anderegg, W.R.L., Wolf, A., Arango-Velez, A., Choat, B., Chmura, D.J., Jansen, S., Kolb, T., Li, S., Meinzer, F.C., Pita, P., Resco de Dios, V., Sperry, J.S., Wolfe, B.T., Pacala, S., 2018. Woody plants optimise stomatal behaviour relative to hydraulic risk. Ecol. Lett. https://doi.org/10.1111/ele.12962
- Barnes, M.L., Biederman, J.A., Farella, M.M., Scott, R.L., Moore, D.J.P., Ponce-Campos, G.E., Biederman, J., MacBean, N., Litvak, M.E., Breshears, D.D., 2021. Improved dryland carbon flux predictions with explicit consideration of water-carbon coupling. Commun. Earth Environ. 2, 248. https://doi.org/10.1038/s43247-021-00308-2
- 518 Beikircher, B., Mayr, S., 2008. The hydraulic architecture of Juniperus communis L. ssp. communis: 519 Shrubs and trees compared. Plant, Cell Environ. 31, 1545–1556. https://doi.org/10.1111/j.1365-520 3040.2008.01860.x
- Biederman, J.A., Scott, R.L., Bell, T.W., Bowling, D.R., Dore, S., Garatuza-Payan, J., Kolb, T.E., Krishnan, P., Krofcheck, D.J., Litvak, M.E., Maurer, G.E., Meyers, T.P., Oechel, W.C., Papuga, S.A., Ponce-Campos, G.E., Rodriguez, J.C., Smith, W.K., Vargas, R., Watts, C.J., Yepez, E.A., Goulden, M.L., 2017. CO2 exchange and evapotranspiration across dryland ecosystems of southwestern North America. Glob. Chang. Biol. 23, 4204–4221. https://doi.org/10.1111/gcb.13686
- Bowling, D.R., Bethers-Marchetti, S., Lunch, C.K., Grote, E.E., Belnap, J., 2010. Carbon, water, and energy fluxes in a semiarid cold desert grassland during and following multiyear drought. J. Geophys. Res. Biogeosciences 115, 1–16. https://doi.org/10.1029/2010JG001322
- 529 Breshears, D.D., Cobb, N.S., Rich, P.M., Price, K.P., Allen, C.D., Balice, R.G., Romme, W.H., Kastens, J.H., 530 Floyd, M.L., Belnap, J., Anderson, J.J., Myers, O.B., Meyer, C.W., 2005. Regional vegetation die-off in response to global-change-type drought. Proc. Natl. Acad. Sci. U. S. A. 102, 15144–15148. https://doi.org/10.1073/pnas.0505734102
- Bunn, A.G., 2008. A dendrochronology program library in R (dplR). Dendrochronologia 26, 115–124. https://doi.org/10.1016/j.dendro.2008.01.002
- Cook, B., Mankin, J., Williams, A., Marvel, K., Smerdon, J., Liu, H., 2021. Uncertainties, Limits, and
   Benefits of Climate Change Mitigation for Soil Moisture Drought in Southwestern North America.
   Earth's Futur. 9, e2021EF002014. https://doi.org/10.1029/2021EF002014
- Ehleringer, J., Schwinning, S., Gebauer, R., 1999. Water use in arid land systems, in: Press, M., Scholes, J., Barker, M. (Eds.), Physiological Plant Ecology. pp. 347–365.
- Eller, C.B., Rowland, L., Mencuccini, M., Rosas, T., Williams, K., Harper, A., Medlyn, B.E., Wagner, Y.,
  Klein, T., Teodoro, G.S., Oliveira, R.S., Matos, I.S., Rosado, B.H.P., Fuchs, K., Wohlfahrt, G.,
  Montagnani, L., Meir, P., Sitch, S., Cox, P.M., 2020. Stomatal optimization based on xylem
  hydraulics (SOX) improves land surface model simulation of vegetation responses to climate. New
  Phytol. 226, 1622–1637. https://doi.org/10.1111/nph.16419
- Feldman, A., Short Gianotti, D., Konings, A., Gentine, P., Entekhabi, D., 2021. Patterns of plant rehydration and growth following pulses of soil moisture availability. Biogeosciences Discuss. 18, 831–847. https://doi.org/10.5194/bg-2020-380
- Feldman, A.F., Chulakadabba, A., Short Gianotti, D.J., Entekhabi, D., 2021. Landscape-Scale Plant Water
   Content and Carbon Flux Behavior Following Moisture Pulses: From Dryland to Mesic
   Environments. Water Resour. Res. 57, 1–20. https://doi.org/10.1029/2020WR027592

- Forzieri, G., Castelli, F., Vivoni, E.R., 2011. Vegetation dynamics within the North American monsoon region. J. Clim. 24, 1763–1783. https://doi.org/10.1175/2010JCLI3847.1
- 553 Fu, Z., Ciais, P., Prentice, I., Gentine, P., Mekowski, D., Bastos, A., Luo, X., Green, J., Stoy, P., Yang, H.,
  554 Hajima, T., 2022. Atmospheric dryness reduces photosynthesis along a large range of soil water
  555 deficits. Nat. Clim. Chang. 13, 989.
- Gebauer, R.L.E., Ehleringer, J.R., 2000. Water and nitrogen uptake patterns following moisture pulses in
   a cold desert community. Ecology 81, 1415–1424. https://doi.org/10.1890/0012 9658(2000)081[1415:WANUPF]2.0.CO;2
- 559 Goulden, M.L., Bales, R.C., 2019. California forest die-off linked to multi-year deep soil drying in 2012–560 2015 drought. Nat. Geosci. https://doi.org/10.1038/s41561-019-0388-5
- Green, J.K., Seneviratne, S.I., Berg, A.M., Findell, K.L., Lawrence, D.M., Gentine, P., 2019. Large influence
   of soil moisture variability on long-term terrestrial carbon uptake. Nature Accepted.
   https://doi.org/10.1038/s41586-018-0848-x
- Grossiord, C., Buckley, T.N., Cernusak, L.A., Novick, K.A., Poulter, B., Siegwolf, R.T.W., Sperry, J.S.,
  McDowell, N.G., 2020. Plant responses to rising vapor pressure deficit. New Phytol. 226, 1550–
  1566. https://doi.org/10.1111/nph.16485
- 567 Guo, J.S., Hultine, K.R., Koch, G.W., Kropp, H., Ogle, K., 2020. Temporal shifts in iso/anisohydry revealed 568 from daily observations of plant water potential in a dominant desert shrub. New Phytol. 225, 713– 569 726. https://doi.org/10.1111/nph.16196
- Humphrey, V., Berg, A., Ciais, P., Gentine, P., Jung, M., Reichstein, M., Seneviratne, S.I., Frankenberg, C., 2021. Soil moisture—atmosphere feedback dominates land carbon uptake variability. Nature 592, 65–69. https://doi.org/10.1038/s41586-021-03325-5
- Huxman, T.E., Cable, J.M., Ignace, D.D., Eilts, J.A., English, N.B., Weltzin, J., Williams, D.G., 2004a.
  Response of net ecosystem gas exchange to a simulated precipitation pulse in a semi-arid grassland: The role of native versus non-native grasses and soil texture. Oecologia 141, 295–305.
  https://doi.org/10.1007/s00442-003-1389-y
- Huxman, T.E., Snyder, K.A., Tissue, D., Leffler, A.J., Ogle, K., Pockman, W.T., Sandquist, D.R., Potts, D.L.,
   Schwinning, S., 2004b. Precipitation pulses and carbon fluxes in semiarid and arid ecosystems.
   Oecologia 141, 254–268. https://doi.org/10.1007/s00442-004-1682-4
- Jain, P., Liu, W., Zhu, S., Chang, C.Y.Y., Melkonian, J., Rockwell, F.E., Pauli, D., Sun, Y., Zipfel, W.R.,
   Michele Holbrook, N., Riha, S.J., Gore, M.A., Stroock, A.D., 2021. A minimally disruptive method for
   measuring water potential in planta using hydrogel nanoreporters. Proc. Natl. Acad. Sci. U. S. A.
   118, 1–9. https://doi.org/10.1073/pnas.2008276118
- Jenerette, G.D., Scott, R.L., Huxman, T.E., 2008. Whole ecosystem metabolic pulses following precipitation events. Funct. Ecol. 22, 924–930. https://doi.org/10.1111/j.1365-2435.2008.01450.x
- Kannenberg, S.A., Bowling, D.R., Anderegg, W.R.L., 2022. AmeriFlux BASE US-CdM Cedar Mesa, Ver. 1-5, AmeriFlux AMP, (Dataset). https://doi.org/https://doi.org/10.17190/AMF/1865477
- Kannenberg, S.A., Bowling, D.R., Anderegg, W.R.L., 2020. Hot moments in ecosystem fluxes: High GPP anomalies exert outsized influence on the carbon cycle and are differentially driven by moisture availability across biomes. Environ. Res. Lett. 15. https://doi.org/10.1088/1748-9326/ab7b97
- Kannenberg, S.A., Driscoll, A.W., Malesky, D., Anderegg, W.R.L., 2021. Rapid and surprising dieback of Utah juniper in the southwestern USA due to acute drought stress. For. Ecol. Manage. 480, 118639.

- 593 https://doi.org/10.1016/j.foreco.2020.118639
- Kennedy, D., Swenson, S., Oleson, K.W., Lawrence, D.M., Fisher, R., da Costa, A.C.L., Gentine, P., 2019.
- Implementing plant hydraulics in the Community Land Model , version 5. J. Adv. Model. Earth Syst.
- 596 11, 485–513. https://doi.org/10.1029/2018MS001500
- Koepke, D.F., Kolb, T.E., 2013. Cavitation at a Forest-Woodland Ecotone. For. Sci. 59, 524–535.
- Kolus, H.R., Huntzinger, D.N., Schwalm, C.R., Fisher, J.B., Mckay, N., Fang, Y., Michalak, A.M., Schaefer,
- K., Wei, Y., Poulter, B., Mao, J., Parazoo, N.C., Shi, X., 2019. Land carbon models underestimate the
- severity and duration of drought's impact on plant productivity. Sci. Rep. 9, 2758.
- 601 https://doi.org/10.1038/s41598-019-39373-1
- Kurc, S.A., Small, E.E., 2007. Soil moisture variations and ecosystem-scale fluxes of water and carbon in
- semiarid grassland and shrubland. Water Resour. Res. 43, 1–13.
- 604 https://doi.org/10.1029/2006WR005011
- Lauenroth, W.K., Bradford, J.B., 2009. Ecohydrology of dry regions of the United States: precipitation pulses and intraseasonal drought. Ecohydrology 2, 173–181. https://doi.org/10.1002/eco
- 607 Liu, L., Gudmundsson, L., Hauser, M., Qin, D., Li, S., Seneviratne, S.I., 2020. Soil moisture dominates dryness stress on ecosystem production globally. Nat. Commun. 11, 1–9.
- 609 https://doi.org/10.1038/s41467-020-18631-1
- MacBean, N., Scott, R.L., Biederman, J.A., Ottlé, C., Vuichard, N., Ducharne, A., Kolb, T., Dore, S., Litvak,
- M., Moore, D.J.P., 2020. Testing water fluxes and storage from two hydrology configurations within
- the ORCHIDEE land surface model across US semi-arid sites. Hydrol. Earth Syst. Sci. 24, 5203–5230.
- 613 https://doi.org/10.5194/hess-24-5203-2020
- MacBean, N., Scott, R.L., Biederman, J.A., Peylin, P., Kolb, T., Litvak, M.E., Krishnan, P., Meyers, T.P.,
- Arora, V.K., Bastrikov, V., Goll, D., Lombardozzi, D.L., Nabel, J.E.M.S., Pongratz, J., Sitch, S., Walker,
- A.P., Zaehle, S., Moore, D.J.P., 2021. Dynamic global vegetation models underestimate net CO2 flux
- 617 mean and inter-annual variability in dryland ecosystems. Environ. Res. Lett. 16.
- 618 https://doi.org/10.1088/1748-9326/ac1a38
- Massman, W., 2000. A simple method for estimating frequency response corrections for eddy
- 620 covariance systems. Agric. For. Meteorol. 104, 185–198.
- McCormick, E.L., Dralle, D.N., Hahm, W.J., Tune, A.K., Schmidt, L.M., Chadwick, K.D., Rempe, D.M., 2021.
- Widespread woody plant use of water stored in bedrock. Nature 597, 225–229.
- 623 https://doi.org/10.1038/s41586-021-03761-3
- Nauman, T.W., Duniway, M.C., 2020. A hybrid approach for predictive soil property mapping using
- 625 conventional soil survey data. Soil Sci. Soc. Am. J. 84, 1170–1194.
- 626 https://doi.org/10.1002/saj2.20080
- Novick, K.A., Biederman, J.A., Desai, A.R., Litvak, M.E., Moore, D.J.P., Scott, R.L., Torn, M.S., 2018. The
- AmeriFlux network: A coalition of the willing. Agric. For. Meteorol. 249, 444–456.
- 629 https://doi.org/10.1016/j.agrformet.2017.10.009
- Novick, K.A., Ficklin, D.L., Baldocchi, D., Davis, K.J., Ghezzehei, T.A., Konings, A.G., MacBean, N., Raoult,
- N., Scott, R.L., Shi, Y., Sulman, B.N., Wood, J.D., 2022. Confronting the water potential information
- 632 gap. Nat. Geosci. 15, 158–164. https://doi.org/10.1038/s41561-022-00909-2
- Novick, K.A., Ficklin, D.L., Stoy, P.C., Williams, C.A., Bohrer, G., Oishi, A.C., Papuga, S.A., Blanken, P.D.,
- Noormets, A., Sulman, B.N., Scott, R.L., Wang, L., Phillips, R.P., 2016. The increasing importance of

atmospheric demand for ecosystem water and carbon fluxes. Nat. Clim. Chang. 6, 1023–1027. https://doi.org/10.1038/nclimate3114

637

678

679

680

Noy-Meir, I., 1973. Desert ecosystems: Environment and producers. Annu. Rev. Ecol. Syst. 4, 25–51.

638 Pastorello, G., Trotta, C., Canfora, E., Chu, H., Christianson, D., Cheah, Y.W., Poindexter, C., Chen, J., 639 Elbashandy, A., Humphrey, M., Isaac, P., Polidori, D., Ribeca, A., van Ingen, C., Zhang, L., Amiro, B., 640 Ammann, C., Arain, M.A., Ardö, J., Arkebauer, T., Arndt, S.K., Arriga, N., Aubinet, M., Aurela, M., 641 Baldocchi, D., Barr, A., Beamesderfer, E., Marchesini, L.B., Bergeron, O., Beringer, J., Bernhofer, C., 642 Berveiller, D., Billesbach, D., Black, T.A., Blanken, P.D., Bohrer, G., Boike, J., Bolstad, P. V., Bonal, D., 643 Bonnefond, J.M., Bowling, D.R., Bracho, R., Brodeur, J., Brümmer, C., Buchmann, N., Burban, B., 644 Burns, S.P., Buysse, P., Cale, P., Cavagna, M., Cellier, P., Chen, S., Chini, I., Christensen, T.R., 645 Cleverly, J., Collalti, A., Consalvo, C., Cook, B.D., Cook, D., Coursolle, C., Cremonese, E., Curtis, P.S., 646 D'Andrea, E., da Rocha, H., Dai, X., Davis, K.J., De Cinti, B., de Grandcourt, A., De Ligne, A., De 647 Oliveira, R.C., Delpierre, N., Desai, A.R., Di Bella, C.M., di Tommasi, P., Dolman, H., Domingo, F., 648 Dong, G., Dore, S., Duce, P., Dufrêne, E., Dunn, A., Dušek, J., Eamus, D., Eichelmann, U., ElKhidir, 649 H.A.M., Eugster, W., Ewenz, C.M., Ewers, B., Famulari, D., Fares, S., Feigenwinter, I., Feitz, A., 650 Fensholt, R., Filippa, G., Fischer, M., Frank, J., Galvagno, M., Gharun, M., Gianelle, D., Gielen, B., 651 Gioli, B., Gitelson, A., Goded, I., Goeckede, M., Goldstein, A.H., Gough, C.M., Goulden, M.L., Graf, 652 A., Griebel, A., Gruening, C., Grünwald, T., Hammerle, A., Han, S., Han, X., Hansen, B.U., Hanson, C., 653 Hatakka, J., He, Y., Hehn, M., Heinesch, B., Hinko-Najera, N., Hörtnagl, L., Hutley, L., Ibrom, A., 654 Ikawa, H., Jackowicz-Korczynski, M., Janouš, D., Jans, W., Jassal, R., Jiang, S., Kato, T., Khomik, M., 655 Klatt, J., Knohl, A., Knox, S., Kobayashi, H., Koerber, G., Kolle, O., Kosugi, Y., Kotani, A., Kowalski, A., 656 Kruijt, B., Kurbatova, J., Kutsch, W.L., Kwon, H., Launiainen, S., Laurila, T., Law, B., Leuning, R., Li, 657 Yingnian, Liddell, M., Limousin, J.M., Lion, M., Liska, A.J., Lohila, A., López-Ballesteros, A., López-658 Blanco, E., Loubet, B., Loustau, D., Lucas-Moffat, A., Lüers, J., Ma, S., Macfarlane, C., Magliulo, V., 659 Maier, R., Mammarella, I., Manca, G., Marcolla, B., Margolis, H.A., Marras, S., Massman, W., 660 Mastepanov, M., Matamala, R., Matthes, J.H., Mazzenga, F., McCaughey, H., McHugh, I., McMillan, 661 A.M.S., Merbold, L., Meyer, W., Meyers, T., Miller, S.D., Minerbi, S., Moderow, U., Monson, R.K., 662 Montagnani, L., Moore, C.E., Moors, E., Moreaux, V., Moureaux, C., Munger, J.W., Nakai, T., 663 Neirynck, J., Nesic, Z., Nicolini, G., Noormets, A., Northwood, M., Nosetto, M., Nouvellon, Y., 664 Novick, K., Oechel, W., Olesen, J.E., Ourcival, J.M., Papuga, S.A., Parmentier, F.J., Paul-Limoges, E., 665 Pavelka, M., Peichl, M., Pendall, E., Phillips, R.P., Pilegaard, K., Pirk, N., Posse, G., Powell, T., Prasse, 666 H., Prober, S.M., Rambal, S., Rannik, Ü., Raz-Yaseef, N., Reed, D., de Dios, V.R., Restrepo-Coupe, N., 667 Reverter, B.R., Roland, M., Sabbatini, S., Sachs, T., Saleska, S.R., Sánchez-Cañete, E.P., Sanchez-668 Mejia, Z.M., Schmid, H.P., Schmidt, M., Schneider, K., Schrader, F., Schroder, I., Scott, R.L., Sedlák, 669 P., Serrano-Ortíz, P., Shao, C., Shi, P., Shironya, I., Siebicke, L., Šigut, L., Silberstein, R., Sirca, C., 670 Spano, D., Steinbrecher, R., Stevens, R.M., Sturtevant, C., Suyker, A., Tagesson, T., Takanashi, S., 671 Tang, Y., Tapper, N., Thom, J., Tiedemann, F., Tomassucci, M., Tuovinen, J.P., Urbanski, S., 672 Valentini, R., van der Molen, M., van Gorsel, E., van Huissteden, K., Varlagin, A., Verfaillie, J., 673 Vesala, T., Vincke, C., Vitale, D., Vygodskaya, N., Walker, J.P., Walter-Shea, E., Wang, H., Weber, R., 674 Westermann, S., Wille, C., Wofsy, S., Wohlfahrt, G., Wolf, S., Woodgate, W., Li, Yuelin, Zampedri, 675 R., Zhang, J., Zhou, G., Zona, D., Agarwal, D., Biraud, S., Torn, M., Papale, D., 2020. The 676 FLUXNET2015 dataset and the ONEFlux processing pipeline for eddy covariance data. Sci. Data 7, 677 225. https://doi.org/10.1038/s41597-020-0534-3

Plaut, J.A., Wadsworth, W.D., Pangle, R., Yepez, E.A., McDowell, N.G., Pockman, W.T., 2013. Reduced transpiration response to precipitation pulses precedes mortality. New Phytol. 200, 375–387.

Poulter, B., Frank, D., Ciais, P., Myneni, R.B., Andela, N., Bi, J., Broquet, G., Canadell, J.G., Chevallier, F.,

- Liu, Y.Y., Running, S.W., Sitch, S., Van Der Werf, G.R., 2014. Contribution of semi-arid ecosystems to interannual variability of the global carbon cycle. Nature 509, 600–603.
- 683 https://doi.org/10.1038/nature13376
- Reichstein, M., Falge, E., Baldocchi, D., Papale, D., Aubinet, M., Berbigier, P., Bernhofer, C., Buchmann, N., Gilmanov, T., Granier, A., Grunwald, T., Havrankova, K., Ilvesniemi, H., Janous, D., Knohl, A.,
- Laurila, T., Lohila, A., Loustau, D., Matteucci, G., Meyers, T., Miglietta, F., Ourcival, J.M., Pumpanen,
- J., Rambal, S., Rotenberg, E., Sanz, M., Tenhunen, J., Seufert, G., Vaccari, F., Vesala, T., Yakir, D.,
- Valentini, R., 2005. On the separation of net ecosystem exchange into assimilation and ecosystem
- respiration: Review and improved algorithm. Glob. Chang. Biol. 11, 1424–1439.
- 690 https://doi.org/10.1111/j.1365-2486.2005.001002.x
- Reynolds, J.F., Kemp, P.R., Ogle, K., Fernández, R.J., 2004. Modifying the "pulse-reserve" paradigm for deserts of North America: Precipitation pulses, soil water, and plant responses. Oecologia 141, 194–210. https://doi.org/10.1007/s00442-004-1524-4
- Reynolds, J.F., Stafford Smith, D.M., Lambin, E.F., Turner, B.L., Mortimore, M., Batterbury, S.P.J., Downing, T.E., Dowlatabadi, H., Fernández, R.J., Herrick, J.E., Huber-Sannwald, E., Jiang, H.,
- Leemans, R., Lynam, T., Maestre, F.T., Ayarza, M., Walker, B., 2007. Global desertification: Building
- a science for dryland development. Science (80-. ). 316, 847–851.
- 698 https://doi.org/10.1126/science.1131634
- Roby, M.C., Scott, R.L., Moore, D.J.P., 2020. High Vapor Pressure Deficit Decreases the Productivity and Water Use Efficiency of Rain-Induced Pulses in Semiarid Ecosystems. J. Geophys. Res.

  Biogeosciences 125, 1–14. https://doi.org/10.1029/2020JG005665
- Sabot, M.E.B., De Kauwe, M.G., Pitman, A.J., Medlyn, B.E., Verhoef, A., Ukkola, A.M., Abramowitz, G.,
   2020. Plant profit maximization improves predictions of European forest responses to drought.
   New Phytol. 226, 1638–1655. https://doi.org/10.1111/nph.16376
- Samuels-Crow, K.E., Ogle, K., Litvak, M.E., 2020. Atmosphere-Soil Interactions Govern Ecosystem Flux
   Sensitivity to Environmental Conditions in Semiarid Woody Ecosystems Over Varying Timescales. J.
   Geophys. Res. Biogeosciences 125, 1–16. https://doi.org/10.1029/2019JG005554
- Schenk, H.J., Espino, S., Goedhart, C.M., Nordenstahl, M., Martinez Cabrera, H.I., Jones, C.S., 2008.
   Hydraulic integration and shrub growth form linked across continental aridity gradients. Proc. Natl.
   Acad. Sci. U. S. A. 105, 11248–11253. https://doi.org/10.1073/pnas.0804294105
- Schwinning, S., Litvak, M.E., Pockman, W.T., Pangle, R.E., Fox, A.M., Huang, C., Mcintire, C.D., 2020. A 3 dimensional model of Pinus edulis and Juniperus monosperma root distributions in New Mexico:
   implications for soil water dynamics. Plant Soil 450, 337–355.
- Schwinning, S., Sala, O.E., 2004. Hierarchy of responses to resource pulses in arid and semi-arid ecosystems. Oecologia 141, 211–220. https://doi.org/10.1007/s00442-004-1520-8
- Seki, K., 2007. SWRC fit a nonlinear fitting program with a water retention curve for soils having unimodal and bimodal pore structure. Hydrol. Earth Syst. Sci. Discuss. 4, 407–437. https://doi.org/10.5194/hessd-4-407-2007
- Siirila-Woodburn, E., Rhoades, A., Hatchett, B., Huning, L., Szinai, J., Tague, C., Nico, P., Feldman, D.,
   Jones, A., Collins, W., Kaatz, L., 2021. A low- to- no snow future and its impacts on water resources in the western United States. Nat. Rev. Earth Environ. https://doi.org/10.1038/s43017-021-00219-
- 722

У

- 723 Smith, W.K., Dannenberg, M.P., Yan, D., Herrmann, S., Barnes, M.L., Barron-Gafford, G.A., Biederman, 724 J.A., Ferrenberg, S., Fox, A.M., Hudson, A.R., Knowles, J.F., MacBean, N., Moore, D.J.P., Nagler, P.L.,
- 725 Reed, S.C., Rutherford, W.A., Scott, R.L., Wang, X., Yang, J., 2019. Remote sensing of dryland
- 726 ecosystem structure and function: Progress, challenges, and opportunities. Remote Sens. Environ.
- 727 233, 111401. https://doi.org/10.1016/j.rse.2019.111401
- 728 Sperry, J.S., Venturas, M.D., Anderegg, W.R.L., Mencuccini, M., Mackay, D.S., Wang, Y., Love, D.M., 2017. 729 Predicting stomatal responses to the environment from the optimization of photosynthetic gain
- 730 and hydraulic cost. Plant Cell Environ. 40, 816-830. https://doi.org/10.1111/pce.12852
- 731 Stocker, B.D., Zscheischler, J., Keenan, T.F., Prentice, I.C., Seneviratne, S.I., Peñuelas, J., 2019. Drought 732 impacts on terrestrial primary production underestimated by satellite monitoring. Nat. Geosci. 12, 733 264-270. https://doi.org/10.1038/s41561-019-0318-6
- 734 Team, R.C., 2022. R: A language and environment for statistical computing.
- 735 Trugman, A.T., Medvigy, D., Mankin, J.S., Anderegg, W.R.L., 2018. Soil Moisture Stress as a Major Driver
- 736 of Carbon Cycle Uncertainty. Geophys. Res. Lett. 45, 6495–6503.
- 737 https://doi.org/10.1029/2018GL078131
- 738 van Genuchten, M.T., 1980. A closed-form equation for predicting the hydraulic conductivity of 739 unsaturated soils. Soil Sci. Soc. Am. J. 44, 892-898.
- 740 https://doi.org/10.2136/sssaj1980.03615995004400050002x
- 741 Vargas, R., Sánchez-Cañete P., E., Serrano-Ortiz, P., Curiel Yuste, J., Domingo, F., López-Ballesteros, A., 742 Oyonarte, C., 2018. Hot-Moments of Soil CO2 Efflux in a Water-Limited Grassland. Soil Syst. 2, 47.
- 743 https://doi.org/10.3390/soilsystems2030047
- 744 Venturas, M.D., Todd, H.N., Trugman, A.T., Anderegg, W.R.L., 2020. Understanding and predicting forest 745 mortality in the western United States using long-term forest inventory data and modeled 746 hydraulic damage. New Phytol. https://doi.org/10.1111/nph.17043
- 747 Verma, M., Friedl, M.A., Richardson, A.D., Kiely, G., Cescatti, A., Law, B.E., Wohlfahrt, G., Gielen, B., 748 Roupsard, O., Moors, E.J., Toscano, P., Vaccari, F.P., Gianelle, D., Bohrer, G., Varlagin, A., 749 Buchmann, N., Van Gorsel, E., Montagnani, L., Propastin, P., 2014. Remote sensing of annual 750 terrestrial gross primary productivity from MODIS: An assessment using the FLUXNET la Thuile data 751 set. Biogeosciences 11, 2185-2200. https://doi.org/10.5194/bg-11-2185-2014
- 752 Vickers, D., Mahrt, L., 1997. Quality Control and Flux Sampling Problems for Tower and Aircraft Data. J. 753 Atmos. Ocean. Technol. 14, 512-526.
- 754 Wang, L., Manzoni, S., Ravi, S., Riveros-Iregui, D., Caylor, K., 2015. Dynamic interactions of 755 ecohydrological and biogeochemical processes in water-limited systems. Ecosphere 6, 1–27. https://doi.org/10.1890/ES15-00122.1 756
- 757 Webb, E., Pearman, G., Leuning, R., 1980. Correction of flux measurements for density effects due to 758 heat and water vapour transfer. Q. J. R. Meteorol. Soc. 106, 85–100.
- 759 West, A.G., Hultine, K.R., Burtch, K.G., Ehleringer, J.R., 2007a. Seasonal variations in moisture use in a 760 piñon-juniper woodland. Oecologia 153, 787–798. https://doi.org/10.1007/s00442-007-0777-0
- 761 West, A.G., Hultine, K.R., Jackson, T.L., Ehleringer, J.R., 2007b. Differential summer water use by Pinus 762 edulis and Juniperus osteosperma reflects contrasting hydraulic characteristics. Tree Physiol. 27, 763 1711–1720. https://doi.org/10.1093/treephys/27.12.1711
- 764 Williams, A.P., Cook, B.I., Smerdon, J.E., 2022. Rapid intensification of the emerging southwestern North

765 766	American megadrought in 2020–2021. Nat. Clim. Chang. 12, 232–234. https://doi.org/10.1038/s41558-022-01290-z
767 768 769	Williams, D.G., Ehleringer, J.R., 2000. Intra- and interspecific variation for summer precipitation use in pinyon-juniper woodlands. Ecol. Monogr. 70, 517–537. https://doi.org/10.1890/0012-9615(2000)070[0517:IAIVFS]2.0.CO;2
770 771 772	Wutzler, T., Lucas-Moffat, A., Migliavacca, M., Knauer, J., Sickel, K., Šigut, L., Menzer, O., Reichstein, M. 2018. Basic and extensible post-processing of eddy covariance flux data with REddyProc. Biogeosciences 15, 5015–5030. https://doi.org/10.5194/bg-15-5015-2018
773	